

**NASA
Technical
Paper
2632**

December 1986

**Theory for Computing the
Field Scattered From a
Smooth Inflected Surface**

**Raymond L. Barger
and Allen K. Dominek**

(NASA-TP-2632) THEORY FOR COMPUTING THE
FIELD SCATTERED FROM A SMOOTH INFLECTED
SURFACE (NASA) 23 p CSCL 20F

N87-13264

Unclas

H1/74 44717

NASA

**NASA
Technical
Paper
2632**

1986

**Theory for Computing the
Field Scattered From a
Smooth Inflected Surface**

Raymond L. Barger
*Langley Research Center
Hampton, Virginia*

Allen K. Dominek
*Ohio State University
Columbus, Ohio*



National Aeronautics
and Space Administration

**Scientific and Technical
Information Branch**

Summary

A theory is described for computing the reflected or scattered field from a smooth body with inflection points. These inflections occur in certain directions at each surface point for which the total (Gaussian) curvature is zero or negative. For surface illumination in one of these critical directions, the usual reflection formulas obtained by the high-frequency approximation are inapplicable, and a shadow zone exists in the reflected field. Scattering into the shadow zone is treated, as well as specular reflection. This theory should have a variety of applications such as for certain optics problems, computer graphics modelling of three-dimensional shapes, and the design and analysis of specialized microwave reflector antennas.

Introduction

When a wave is incident on a smooth surface, the reflected field can usually be computed, in the high-frequency approximation, provided that the curvature distribution of the surface in the vicinity of the reflection point is known. For the monostatic case (receiver coincident with source), the two principal curvatures are required. For the bistatic case, the curvature in the direction of the incidence plane is required as well as the curvature in the orthogonal direction. If one of these curvatures is zero, the usual formula is inapplicable. This problem is caused by the vanishing of the quadratic term in the local phase distribution function. The next higher order nonvanishing term must be included in the surface current integration to obtain the high-frequency approximation for the scattered field. In this analysis, it is assumed that this term is the cubic term.

A special case of inflection point scattering has been treated in reference 1. The analysis of reference 1 is limited to reflection from bodies of revolution in a system configured in such a way that the body surface equation is expressed in a coordinate system whose origin is located at the ray source.

Such a restricted analysis cannot be applied to more general configurations. For a body of revolution, all the required surface geometric parameters are readily obtained from the equation of the meridian line, but for more general surfaces this simplification is not available. Even for an axisymmetric surface, it would not be a trivial matter to adapt the analysis of reference 1 to the situation in which the body is illuminated from an off-axis source, especially if, for the bistatic case, the incidence reflection plane does not intersect the body axis.

The present analysis is not restricted to axisymmetric shapes or to a special coordinate system. However, the analysis is limited to the far-field condition, primarily for clarity in presentation of the concepts. Modification of the analysis to account for near-field conditions should be fairly straightforward.

Symbols

A, B, a, b	parameters defined by equations (37) through (40)
$Ai[]$	Airy function
c	proportionality constant used in derivation of equation (7)
\mathbf{E}	electric field vector
E	component of \mathbf{E}
E, F, G	metric coefficients evaluated at \mathbf{r}_0

e, f, g	curvature parameters evaluated at \mathbf{r}_o
e	unit base vector
e_{Ts}	unit vector with direction of vector projection of \hat{I}_s onto tangent plane
e_θ	unit vector $\hat{e}_\perp \times \hat{I}_i$ (see fig. 3)
$e_{\theta s}$	unit vector in scattering plane orthogonal to \hat{I}_s (see fig. 3)
e_\parallel	$= \hat{N} \times \hat{e}_\perp$
e_\perp	unit vector orthogonal to incidence plane
$e_{\perp s}$	unit vector orthogonal to scattering plane
\mathbf{H}	magnetic field vector
H	component of \mathbf{H}
I	ray direction vector
I_a	direction of $\hat{I}_s - \hat{I}_i$
I_p	vector projection of \hat{I}_i onto tangent plane
\mathbf{J}_p	projection of surface current field onto polarization plane of scattered ray
J	component of \mathbf{J}_p
j	$= \sqrt{-1}$
k	wave number
m	magnitude
\hat{N}	local surface normal direction vector
$\mathbf{P}_i, \mathbf{P}_s$	projection operators defined by equations (50) and (51)
\mathbf{R}	rotation matrix
R	distance from \mathbf{r}_o in direction \hat{I}_s
\mathbf{r}	surface vector
\mathbf{r}_o	point of ray incidence on surface
S	surface area
s	distance along arc on surface
s_\perp^*	variable defined by equation (42)
u, v	independent surface variables
ζ	local distance of surface from tangent plane at \mathbf{r}_o
η, ξ	local surface variable, varying in \hat{e}_\perp or \hat{e}_\parallel direction, respectively

θ	angle of incidence
θ_s	scattering angle
θ^*	angle between \hat{I}_a and \hat{N} , $\cos \theta^* = \hat{N} \cdot \hat{I}_a$
κ	normal curvature of surface
λ	direction of surface arc at \mathbf{r}_o as indicated by dv/du on arc
μ	permeability
Φ	phase
ϕ_s	angle between \hat{e}_{Ts} and \hat{e}_{\parallel}
ϕ_{\parallel}	angle between \hat{I}_a and \hat{e}_{\parallel}
ϕ_{\perp}	angle between \hat{I}_a and \hat{e}_{\perp}
ω	circular frequency
Subscripts:	
i	incidence
s	scattering
θ	component in direction defined by intersection of incident plane with plane normal to incident ray
u, v, ξ, η	partial differentiation with respect to u, v, ξ , and η , respectively
\parallel, \perp	parallel to or orthogonal to incidence plane, respectively

Reflection Shadows Created by Surface Inflection

Figure 1 shows the shape of a body of revolution whose meridian line contains two inflection points. Arrows indicating the incident beam direction and the distribution of reflection directions demonstrate the existence of a reflection shadow region both for the monostatic case (fig. 1(a)) and for the bistatic case (fig. 1(b)).

Figure 2 shows the distribution of specular directions for this body. It is seen that when the incident ray direction is near the horizontal, there is only one specular point. When it is near vertical, there are three specular points. These two regions are separated by the inflection points.

These considerations apply, for purposes of illustration, to the axisymmetric shape illustrated in figure 1. The following analysis is not limited to axisymmetric shapes, however, but applies to arbitrary smooth shapes that are representable as a vector function of two surface variables, $\mathbf{r} = \mathbf{r}(u, v)$. A useful class of such surfaces is described in reference 2. The analysis represents, in some sense, a generalization of the analysis of reference 1. Another approach might be to treat the inflection condition as approximately representable as a near confluence of two reflection points and develop the analysis as in reference 3.

Analysis

Local Surface Geometry

Consider a body illuminated by a plane wave propagating in direction \hat{I}_i . The scattered field received by a far-field observer in direction \hat{I}_s is determined primarily by the local surface geometry near point \mathbf{r}_o at which the surface normal \hat{N} satisfies the reflection condition

$$\hat{I}_s = \hat{I}_i - 2(\hat{I}_i \cdot \hat{N})\hat{N} \quad (1)$$

If the surface is described as a vector function of two variables, $\mathbf{r} = \mathbf{r}(u, v)$, then \hat{N} is the direction of $\mathbf{r}_u \times \mathbf{r}_v$. The local approximation to the surface at \mathbf{r}_o is

$$\begin{aligned} \mathbf{r} = \mathbf{r}_o &+ (\mathbf{r}_u du + \mathbf{r}_v dv) + \frac{1}{2}(\mathbf{r}_{uu} dv^2 \\ &+ 2\mathbf{r}_{uv} du dv + \mathbf{r}_{vv} dv^2) + \frac{1}{3!}(\mathbf{r}_{uuu} du^3 \\ &+ 3\mathbf{r}_{uuv} du^2 dv + 3\mathbf{r}_{uvv} du dv^2 + \mathbf{r}_{vvv} dv^3) \end{aligned} \quad (2)$$

The local shape of the surface is determined by its deviation from the tangent plane, that is, by the component of $\mathbf{r} - \mathbf{r}_o$ normal to the tangent plane,

$$(\mathbf{r} - \mathbf{r}_o) \cdot \hat{N} = \frac{1}{2}(\mathbf{r}_{uu} \cdot \hat{N} du^2 + 2\mathbf{r}_{uv} \cdot \hat{N} du dv + \mathbf{r}_{vv} \cdot \hat{N} dv^2) + \dots \quad (3a)$$

The linear terms

$$\mathbf{r}_u \cdot \hat{N} = \mathbf{r}_v \cdot \hat{N} = 0$$

since \mathbf{r}_u and \mathbf{r}_v lie in the tangent plane. Equation (3a) can now be written as

$$(\mathbf{r} - \mathbf{r}_o) \cdot \hat{N} = \frac{1}{2}(e du^2 + 2f du dv + g dv^2) \quad (3b)$$

where e , f , and g are the curvature parameters defined as

$$e = \mathbf{r}_{uu} \cdot \hat{N}$$

$$f = \mathbf{r}_{uv} \cdot \hat{N}$$

$$g = \mathbf{r}_{vv} \cdot \hat{N}$$

The incremental arc length is given by the formula (ref. 4, p. 58)

$$ds^2 = E du^2 + 2F du dv + G dv^2 \quad (4)$$

Here E , F , and G are the metric coefficients defined as

$$E = \mathbf{r}_u \cdot \mathbf{r}_u$$

$$F = \mathbf{r}_u \cdot \mathbf{r}_v$$

$$G = \mathbf{r}_v \cdot \mathbf{r}_v$$

If a direction is specified on the surface at \mathbf{r}_o by fixing the slope $\lambda = dv/du$, the normal curvature in direction λ is

$$\kappa_\lambda = \frac{(e + 2f\lambda + g\lambda^2) du^2}{(ds/du)^2 du^2} = \frac{e + 2f\lambda + g\lambda^2}{E + 2F\lambda + G\lambda^2} \quad (5)$$

The directions for which κ_λ attains its extreme values are the roots of the quadratic equation

$$\begin{vmatrix} \lambda^2 & -\lambda & 1 \\ E & F & G \\ e & f & g \end{vmatrix} = 0 \quad (6)$$

(See ref. 4, p. 80.) These are the principal curvature directions, and they are mutually orthogonal (ref. 4, p. 80). The maximum and minimum values of normal curvature obtained by substituting these roots into equation (5) are called the principal curvatures.

The direction λ_{\parallel} in which the incidence plane intersects the surface at \mathbf{r}_o (see fig. 3) can be found by projecting the incident ray vector onto the tangent plane

$$\hat{I}_p = \frac{\hat{I}_i - (\hat{I}_i \cdot \hat{N}) \hat{N}}{|\hat{I}_i - (\hat{I}_i \cdot \hat{N}) \hat{N}|}$$

This vector is proportional to $\mathbf{r}_u + \mathbf{r}_v \lambda_{\parallel}$:

$$\hat{I}_p = c(\mathbf{r}_u + \mathbf{r}_v \lambda_{\parallel})$$

Thus, dividing the scalar products

$$\hat{I}_p \cdot \mathbf{r}_u = c(\mathbf{r}_u^2 + \mathbf{r}_u \cdot \mathbf{r}_v \lambda_{\parallel})$$

$$\hat{I}_p \cdot \mathbf{r}_v = c(\mathbf{r}_u \cdot \mathbf{r}_v + \mathbf{r}_v^2 \lambda_{\parallel})$$

and solving for λ_{\parallel} yields

$$\lambda_{\parallel} = \frac{(\hat{I}_p \cdot \mathbf{r}_v) \mathbf{r}_u^2 - (\hat{I}_p \cdot \mathbf{r}_u) (\mathbf{r}_u \cdot \mathbf{r}_v)}{(\hat{I}_p \cdot \mathbf{r}_u) \mathbf{r}_v^2 - (\hat{I}_p \cdot \mathbf{r}_v) (\mathbf{r}_u \cdot \mathbf{r}_v)} \quad (7)$$

The direction λ_{\perp} orthogonal to λ_{\parallel} is given by the formula (ref. 4, p. 59)

$$\lambda_{\perp} = -\frac{(E + F\lambda_{\parallel})}{(F + G\lambda_{\parallel})} \quad (8)$$

Now new local coordinates are defined by the relations

$$d\eta = dv - \lambda_{\parallel} du \quad (9a)$$

$$d\xi = dv - \lambda_{\perp} du \quad (9b)$$

or

$$du = \frac{d\eta - d\xi}{\lambda_{\perp} - \lambda_{\parallel}} \quad (10a)$$

$$dv = \frac{\lambda_{\perp} d\eta - \lambda_{\parallel} d\xi}{\lambda_{\perp} - \lambda_{\parallel}} \quad (10b)$$

Denote the unit base vectors in the tangent plane in directions λ_{\parallel} and λ_{\perp} , by \hat{e}_{\parallel} and \hat{e}_{\perp} , respectively. Thus, ξ varies in the \hat{e}_{\parallel} direction and η varies in the \hat{e}_{\perp} direction. To be more precise, ξ varies along a curve formed by the intersection of the incidence plane with the surface, and η varies along a curve formed by the intersection of the plane of \hat{N} and \hat{e}_{\perp} with the surface. For these curves, the curvature vector at \mathbf{r}_o is in the \hat{N} direction when the curvature is not zero. If the curvature is zero, the vector $d^3\mathbf{r}/ds^3$ points in the \hat{N} direction. Arc length in the \hat{e}_{\parallel} direction is given by

$$\begin{aligned} \frac{ds}{d\xi} d\xi &= \sqrt{E + 2F\lambda_{\parallel} + G\lambda_{\parallel}^2} \frac{du}{d\xi} d\xi \\ ds_{\parallel} &= \frac{\sqrt{E + 2F\lambda_{\parallel} + G\lambda_{\parallel}^2}}{\lambda_{\parallel} - \lambda_{\perp}} d\xi \end{aligned} \quad (11a)$$

Similarly, in the \hat{e}_{\perp} direction,

$$ds_{\perp} = \frac{\sqrt{E + 2F\lambda_{\perp} + G\lambda_{\perp}^2}}{\lambda_{\perp} - \lambda_{\parallel}} d\eta \quad (11b)$$

Scattered Field Calculation

According to reference 5 (p. 149), the field scattered in direction \hat{I}_s is obtained by integrating the physical optics surface current distribution:

$$\mathbf{E}_s = \frac{-j\omega\mu}{2\pi R} e^{-jkR} \int \left[\hat{N} \times \mathbf{H}_i - (\hat{N} \times \hat{\mathbf{H}}_i \cdot \hat{I}_s) \hat{I}_s \right] e^{jkr \cdot (\hat{I}_s - \hat{I}_i)} dS \quad (12)$$

The phase function

$$\Phi = k\mathbf{r}(\xi, \eta) \cdot (\hat{I}_s - \hat{I}_i) \quad (13)$$

is expanded first in the \hat{e}_{\parallel} direction, taking the ξ, η origin at the point of incidence, to give

$$\frac{\Phi}{k} \approx \left[\mathbf{r}(\eta) + \mathbf{r}_{\xi}\xi + \frac{1}{2}\mathbf{r}_{\xi\xi}\xi^2 + \frac{1}{3!}\mathbf{r}_{\xi\xi\xi}\xi^3 \right] \cdot (\hat{I}_s - \hat{I}_i) \quad (14)$$

In the \hat{e}_{\parallel} direction, the surface vector can be written, approximately, as

$$\mathbf{r} - \mathbf{r}_o(\eta) = ds_{\parallel}\hat{e}_{\parallel} + \zeta(\xi)\hat{N} \quad (15)$$

where ζ is the distance of the surface from the tangent plane. Thus,

$$\zeta(o) = \zeta_{\xi}(o) = 0$$

For simple monostatic or bistatic reflection

$$\hat{I}_s - \hat{I}_i = 2 \cos \theta \hat{N}$$

Thus, for this case, the linear term is

$$\mathbf{r}_\xi \cdot (\hat{I}_s - \hat{I}_i) d\xi = 0 \quad (16)$$

The dot product in the quadratic term of the phase expansion becomes

$$\frac{1}{2} \mathbf{r}_{\xi\xi} \cdot (\hat{I}_s - \hat{I}_i) = \mathbf{r}_{\xi\xi} \cdot \hat{N} \cos \theta \quad (17)$$

If $\mathbf{r}_{\xi\xi}(\xi)$ is not identically zero, the remaining terms can be neglected, and the integration with respect to ξ can be carried out by the stationary phase approximation.

Now, considering the term $\mathbf{r}(\eta) \cdot (\hat{I}_s - \hat{I}_i)$ in equation (14), similar considerations apply

$$\mathbf{r}(\eta) = \mathbf{r}_o + \mathbf{r}_\eta d\eta + \frac{1}{2} \mathbf{r}_{\eta\eta} d\eta^2 + \frac{1}{3!} \mathbf{r}_{\eta\eta\eta} d\eta^3 + \dots \quad (18a)$$

$$\mathbf{r}(\eta) = \mathbf{r}_o + ds \hat{e}_\perp + \zeta(\eta) \hat{N} \quad (18b)$$

where $\zeta(0) = \zeta_\eta(0) = 0$. Thus for simple reflection,

$$\mathbf{r}_\eta \cdot (\hat{I}_s - \hat{I}_i) = 0 \quad (19)$$

$$\frac{1}{2} \mathbf{r}_{\eta\eta} \cdot (\hat{I}_s - \hat{I}_i) = \hat{r}_{\eta\eta} \cdot \hat{N} \cos \theta \quad (20)$$

These expressions can be written in terms of the original surface variables u, v as follows:

$$\mathbf{r}_\eta = \mathbf{r}_u u_\eta + \mathbf{r}_v v_\eta = \frac{\mathbf{r}_u + \lambda_\perp \mathbf{r}_v}{\lambda_\perp - \lambda_\parallel} \quad (21)$$

$$\left(\frac{ds_\perp}{d\eta} \right)^2 = \mathbf{r}_\eta \cdot \mathbf{r}_\eta = \frac{E + 2F\lambda_\perp + G\lambda_\perp^2}{(\lambda_\perp - \lambda_\parallel)^2} \quad (22)$$

$$\mathbf{r}_{\eta\eta} = \mathbf{r}_{uu} u_\eta^2 + 2\mathbf{r}_{uv} u_\eta v_\eta + \mathbf{r}_{vv} v_\eta^2 = \frac{\mathbf{r}_{uu} + 2\mathbf{r}_{uv} \lambda_\perp + \mathbf{r}_{vv} \lambda_\perp^2}{(\lambda_\perp - \lambda_\parallel)^2} \quad (23)$$

Now, by definition of the curvature coefficients,

$$\mathbf{r}_{\eta\eta} \cdot \hat{N} = \frac{e + 2f\lambda_\perp + g\lambda_\perp^2}{(\lambda_\perp - \lambda_\parallel)^2} \quad (24a)$$

$$\mathbf{r}_{\eta\eta} \cdot \hat{N} = \frac{e + 2f\lambda_\perp + g\lambda_\perp^2}{E + 2F\lambda_\perp + G\lambda_\perp^2} \left(\frac{ds_\perp}{d\eta} \right)^2 \quad (24b)$$

$$\mathbf{r}_{\eta\eta} \cdot \hat{N} = \kappa_{\perp} \left(\frac{ds_{\perp}}{d\eta} \right)^2 \quad (24c)$$

The quadratic term in the phase function (eq. (20)), therefore, becomes

$$\mathbf{r}_{\eta\eta} \cdot \hat{N} \cos \theta \eta^2 = \kappa_{\perp} \cos \theta \left(\frac{ds_{\perp}}{d\eta} \right)^2 \eta^2 \quad (25)$$

Relations analogous to equations (21) through (25) could also be written for the variation in the \hat{e}_{\parallel} direction to yield

$$\frac{1}{2} \mathbf{r}_{\xi\xi} \cdot (\hat{I}_s - \hat{I}_i) \xi^2 = \kappa_{\parallel} \cos \theta \left(\frac{ds_{\parallel}}{d\xi} \right)^2 \xi^2 \quad (26)$$

or, locally near the stationary point,

$$\frac{1}{2} \mathbf{r}_{\xi\xi} \cdot (\hat{I}_s - \hat{I}_i) \xi^2 = \kappa_{\parallel} \cos \theta s_{\parallel}^2$$

Assuming that the dominant contribution to the integral of equation (12) comes from the stationary point \mathbf{r}_o and removing the surface current from the integral leave the following integral to be evaluated:

$$\begin{aligned} \int e^{jk\mathbf{r}_o \cdot (\hat{I}_s - \hat{I}_i)} dS &\approx e^{jk\mathbf{r}_o \cdot (\hat{I}_s - \hat{I}_i)} \int_{-\infty}^{\infty} \int_{-\infty}^{\infty} e^{jk\kappa_{\perp} \cos \theta s_{\perp}^2} ds_{\perp} \\ &\times e^{jk\kappa_{\parallel} \cos \theta s_{\parallel}^2} ds_{\parallel} = j e^{jk\mathbf{r}_o \cdot (\hat{I}_s - \hat{I}_i)} \frac{\pi}{k \cos \theta} \frac{1}{\sqrt{k_{\perp} \kappa_{\parallel}}} \end{aligned} \quad (27)$$

where the stationary phase approximation has been used to evaluate both integrals.

Now, the surface current is resolved into components:

$$\hat{N} \times \mathbf{H}_i \cdot \hat{e}_{\parallel} = (\hat{N} \times H_{i\perp} \hat{e}_{\perp}) \cdot \hat{e}_{\parallel} = H_{i\perp} \quad (28a)$$

$$\hat{N} \times \mathbf{H}_i \cdot \hat{e}_{\perp} = (\hat{N} \times H_{i\theta} \hat{e}_{\theta}) \cdot \hat{e}_{\perp} = H_{i\theta} \sin(\hat{N}, \hat{e}_{\theta}) = -H_{i\theta} \cos \theta \quad (28b)$$

$$\hat{e}_{\theta} = \hat{e}_{\perp} \times \hat{I}_i \quad (29)$$

Equations (28) give the surface current as

$$\hat{N} \times \mathbf{H}_i = H_{i\perp} \hat{e}_{\parallel} - H_{i\theta} \cos \theta \hat{e}_{\perp} \quad (30)$$

For the reflection direction \hat{I}_s , the projection of $\hat{N} \times \mathbf{H}_i$ onto the polarization plane yields the following components:

$$(\hat{H}_{i\perp} \hat{e}_{\parallel} \cdot \hat{e}_{\theta}) \hat{e}_{\theta} = H_{i\perp} \cos \theta \hat{e}_{\theta} \quad (31a)$$

$$\left(H_{i\theta} \cos \theta \hat{e}_\perp \cdot \hat{e}_\perp \right) \hat{e}_\perp = -H_{i\theta} \cos \theta \hat{e}_\perp \quad (31b)$$

Substituting **E** field components in equations (31a) and (31b) by the relations

$$H_{i\perp} = \frac{k}{\omega\mu} E_{i\theta} \quad (32a)$$

$$H_{i\theta} = \frac{k}{\omega\mu} E_{i\perp} \quad (32b)$$

and using the results together with equation (27) in equation (12) yield

$$\begin{pmatrix} E_{\theta s} \\ E_{\perp s} \end{pmatrix} = \frac{e^{-jkR}}{2R} \frac{e^{jk\mathbf{r}_o \cdot (\hat{I}_s - \hat{I}_i)}}{\sqrt{\kappa_\perp \kappa_\parallel}} \begin{pmatrix} E_{i\theta} \\ -E_{i\perp} \end{pmatrix} \quad (33)$$

This well-known result has been developed in this paper in this manner in order to demonstrate the analytical relationship of this result with that for inflection scattering which is given in the following section.

Reflection at an Inflection Point

The preceding analysis fails if either κ_\perp or κ_\parallel vanishes, that is, if the surface is inflected at \mathbf{r}_o either in the direction of the incidence plane or orthogonal to it. According to equations (24a) and (24b) (or the equivalent equations for ξ variation) this means that for $\lambda = \lambda_\perp$ or $\lambda = \lambda_\parallel$,

$$e + 2f\lambda + g\lambda^2 = 0 \quad (34)$$

This equation has solutions

$$\lambda = \frac{-f \pm \sqrt{f^2 - eg}}{g} \quad (35)$$

Thus, if $eg - f^2 > 0$, equation (34) has no real root. The surface is convex or concave in all directions at \mathbf{r}_o , which is termed an elliptic point. If $eg - f^2 = 0$, equation (34) has one real root, $\lambda = -f/g$, and \mathbf{r}_o is a parabolic point. The surface is inflected in one direction only. If $eg - f^2 < 0$, equation (35) has two real roots corresponding to two directions in which the surface is inflected. In this case, \mathbf{r}_o is a hyperbolic point. Directions λ for which equation (35) is satisfied are called asymptotic directions. If a wave is incident at a hyperbolic point so that the incidence plane is aligned with either of the asymptotic directions, or is orthogonal to either of them, equation (33) fails. For a parabolic point, only two incidence plane directions present this problem.

When the problem does occur, a shadow region is created in the reflected ray tube. This effect was mentioned in the first section and illustrated in figure 1. By differentiating the reflection condition (eq. (1)),

$$\frac{-d\hat{I}_s}{ds} = 2 \left(\hat{I}_i \cdot \hat{N} \right) \frac{d\hat{N}}{ds} + 2 \left(\hat{I}_i \cdot \frac{d\hat{N}}{ds} \right) \hat{N}$$

it is seen that an extreme value of \hat{I}_s is attained for $d\hat{I}/ds = 0$ which occurs when $d\hat{N}/ds = 0$, corresponding to the inflection condition. Thus, the ray reflected at the

$$\frac{k}{2} \mathbf{r}_{\eta\eta} \cdot (\hat{I}_s - \hat{I}_i) \equiv a \quad (40b)$$

where relation (24c) has been used in equation (40a).

With this notation, the integral (corresponding to eq. (27)) to be evaluated is

$$\begin{aligned} \int e^{jk\mathbf{r} \cdot (\hat{I}_s - \hat{I}_i)} dS &= e^{jk\mathbf{r}_o \cdot (\hat{I}_s - \hat{I}_i)} ds_{\parallel} \int_{-\infty}^{\infty} ds_{\perp} \\ &\times \int_{-\infty}^{\infty} e^{j(as_{\perp}^2 + bs_{\perp})} ds_{\perp} e^{j(As_{\parallel}^3 + Bs_{\parallel})} ds_{\parallel} \end{aligned} \quad (41)$$

The inner integral is reduced to the previous type by the simple change of variable:

$$s_{\perp}^* = s_{\perp} + \frac{b}{2a} \quad (42)$$

Equation (41) then yields the result

$$\begin{aligned} &e^{jk\mathbf{r}_o \cdot (\hat{I}_s - \hat{I}_i)} e^{-jb^2/4a} \int_{-\infty}^{\infty} \int_{-\infty}^{\infty} e^{jas_{\perp}^{*2}} ds_{\perp}^* e^{j(As_{\parallel}^3 + Bs_{\parallel})} ds_{\parallel} \\ &= e^{jk\mathbf{r}_o \cdot (\hat{I}_s - \hat{I}_i)} e^{-jb^2/4a} e^{-j\pi/4} \sqrt{\frac{\pi}{a}} \frac{2\pi}{(3A)^{1/3}} Ai \left[\frac{B}{(3A)^{1/3}} \right] \end{aligned} \quad (43a)$$

$$\begin{aligned} &e^{jk\mathbf{r}_o \cdot (\hat{I}_s - \hat{I}_i)} e^{-jb^2/4a} \int_{-\infty}^{\infty} \int_{-\infty}^{\infty} e^{jas_{\perp}^{*2}} ds_{\perp}^* e^{j(As_{\parallel}^3 + Bs_{\parallel})} ds_{\parallel} \\ &= e^{jk\mathbf{r}_o \cdot (\hat{I}_s - \hat{I}_i)} e^{-jb^2/4a} \left(e^{-j\pi/4} \sqrt{\frac{2\pi}{km\kappa_{\perp} \cos \theta^*}} \right) \frac{2\pi}{(3A)^{1/3}} Ai \left[\frac{B}{(3A)^{1/3}} \right] \end{aligned} \quad (43b)$$

where the integrations have been evaluated by the usual formulas (ref. 6, p. 447).

According to equations (28a) and (28b), the surface current is proportional to

$$\hat{N} \times \mathbf{H}_i = (H_{i\perp} \hat{e}_{\parallel} - H_{i\theta} \cos \theta \hat{e}_{\perp}) \quad (44)$$

Resolving the scattering direction vector \hat{I}_s into components in, and normal to, the tangent plane yields

$$\hat{I}_s = \sin \theta_s \hat{e}_{T_s} + \cos \theta_s \hat{N} \quad (45)$$

where

$$\hat{e}_{T_s} = \cos \phi_s \hat{e}_{\parallel} + \sin \phi_s \hat{e}_{\perp} \quad (46)$$

Orthonormal field directions in the polarization plane associated with the scattering direction \hat{I}_s are

$$\hat{e}_{\theta_s} = -\cos \theta_s \hat{e}_{T_s} + \sin \theta_s \hat{N} \quad (47)$$

$$\hat{e}_{\perp s} = -\sin \phi_s \hat{e}_{\parallel} + \cos \phi_s \hat{e}_{\perp} \quad (48)$$

Therefore, the component of the surface current field in the polarization plane is

$$\begin{aligned}
\mathbf{J}_p &\equiv \hat{N} \times \mathbf{H}_i - (\hat{N} \times \mathbf{H}_i \cdot \hat{I}_s) \hat{I}_s \\
&= (-H_{i\perp} \sin \phi_s - H_{i\theta} \cos \theta \cos \phi_s) \hat{e}_{\perp s} \\
&\quad - \cos \theta_s (\cos \phi_s H_{i\perp} - \sin \phi_s \cos \theta H_{i\theta}) \hat{e}_{\theta s} \\
&= \frac{k}{\omega \mu} [(-E_{i\theta} \sin \phi_s + E_{i\perp} \cos \theta \cos \phi_s) \hat{e}_{\perp s} - \cos \theta_s (\cos \phi_s E_{i\theta} \\
&\quad + \sin \phi_s \cos \theta E_{i\perp}) \hat{e}_{\theta s}]
\end{aligned} \tag{49}$$

where relations (32a) and (32b) have been utilized. The matrix operators \mathbf{P}_i , \mathbf{P}_s , and \mathbf{R} are defined as follows:

$$\mathbf{P}_i \equiv \begin{pmatrix} 1 & 0 \\ 0 & \cos \theta \end{pmatrix} \tag{50}$$

$$\mathbf{P}_s \equiv \begin{pmatrix} -\cos \theta_s & 0 \\ 0 & 1 \end{pmatrix} \tag{51}$$

$$\mathbf{R} \equiv \begin{pmatrix} \cos \phi_s & \sin \phi_s \\ -\sin \phi_s & \cos \phi_s \end{pmatrix} \tag{52}$$

The operator \mathbf{P}_i projects from the incident polarization plane to the tangent plane. The operator \mathbf{R} rotates in the tangent plane from the \hat{e}_{\parallel} direction to the \hat{e}_{Ts} direction aligned with the scattering plane. Then the operator \mathbf{P}_s projects from the tangent plane to the polarization plane associated with the scattering direction \hat{I}_s . With equations (50) through (52), equation (49) becomes

$$\begin{pmatrix} J_{\theta s} \\ J_{\perp s} \end{pmatrix} = \frac{k}{\omega \mu} \mathbf{P}_s \mathbf{R} \mathbf{P}_i \begin{pmatrix} E_{i\theta} \\ E_{i\perp} \end{pmatrix} \tag{53}$$

Substituting from equations (43b) and (53) into equation (12) yields the final result as

$$\begin{aligned}
\begin{pmatrix} E_{\theta s} \\ E_{\perp s} \end{pmatrix} &= \frac{e^{-jkR}}{R} e^{i\pi/4} e^{-jb^2/4a} \sqrt{\frac{2\pi k}{m\kappa_{\perp} \cos \theta^*}} e^{j\mathbf{k}\mathbf{r}_o \cdot (\hat{I}_s - \hat{I}_i)} \\
&\times \frac{1}{(3/A)^{1/3}} Ai \left[\frac{B}{(3A)^{1/3}} \right] \mathbf{P}_s \mathbf{R} \mathbf{P}_i \begin{pmatrix} E_{i\theta} \\ E_{i\perp} \end{pmatrix}
\end{aligned} \tag{54}$$

where B , A , b , and a are defined, respectively, by equations (37), (38), (39), and (40). If scattering only in the incidence-reflection plane is considered,

$$\sin \theta^* = 0$$

consequently,

$$b = 0$$

and the factor $e^{-jb^2/4a}$ drops out of equation (54). In this case, the well-known inverse square-root dependence on the normal curvature κ_{\perp} is obtained. However, if scattering outside the incidence reflection plane is considered,

$$e^{-jb^2/4a} \neq 1$$

inflection point \mathbf{r}_o represents the edge of the shadow region. As was mentioned earlier, the field scattered into this shadow region is significant. In order to calculate it from the surface current integral (eq. (12)), the cubic term must be included in the expansion of the phase function in the inflection direction, and scattering directions different from the reflection direction must be considered.

Assume that the surface is inflected at \mathbf{r}_o in the \hat{e}_{\parallel} direction. Then, in the phase function expansion (eq. (14)), the quadratic term vanishes. Since the reflection condition is no longer assumed, equation (1) is no longer applicable. Let \hat{I}_a denote the direction of $I_s - \hat{I}_i$ and m denote its magnitude. Then $\hat{I}_s - \hat{I}_i$ can be resolved into components:

$$\hat{I}_s - \hat{I}_i = m\hat{I}_a = m \left(\cos \theta^* \hat{N} + \cos \phi_{\perp} \hat{e}_{\perp} + \cos \phi_{\parallel} \hat{e}_{\parallel} \right) \quad (36)$$

Since, from equation (15), $\mathbf{r}_{\xi}(o) = \hat{e}_{\parallel}$, the linear term in the phase function becomes

$$k\mathbf{r}_{\xi} \cdot (\hat{I}_s - \hat{I}_i) d\xi = km \cos \phi_{\parallel} ds_{\parallel} \quad (37a)$$

$$k\mathbf{r}_{\xi} \cdot (\hat{I}_s - \hat{I}_i) d\xi \equiv B ds_{\parallel} \quad (37b)$$

or locally,

$$k\mathbf{r}_{\xi} \cdot (\hat{I}_s - \hat{I}_i) d\xi \equiv Bs_{\parallel} \quad (37c)$$

Differentiating equation (15) three times and using equation (36) yields for the cubic term,

$$k\mathbf{r}_{\xi\xi\xi} \cdot (\hat{I}_s - \hat{I}_i) \xi^3 = k \left(\mathbf{r}_{\xi\xi\xi} \cdot \hat{N} \right) m \cos \theta^* \xi^3 \quad (38a)$$

$$k\mathbf{r}_{\xi\xi\xi} \cdot (\hat{I}_s - \hat{I}_i) \xi^3 = k \frac{d\kappa_{\parallel}}{ds_{\parallel}} m \cos \theta^* s_{\parallel}^3 \quad (38b)$$

$$k\mathbf{r}_{\xi\xi\xi} \cdot (\hat{I}_s - \hat{I}_i) \xi^3 \equiv As_{\parallel}^3 \quad (38c)$$

Now, considering the phase variation in the \hat{e}_{\perp} direction, equation (19) is replaced by

$$k \frac{d\mathbf{r}}{ds_{\perp}} \cdot (\hat{I}_s - \hat{I}_i) = km \cos \phi_{\perp} \quad (39a)$$

$$k \frac{d\mathbf{r}}{ds_{\perp}} \cdot (\hat{I}_s - \hat{I}_i) = b \quad (39b)$$

Equation (20) for the quadratic term is replaced by

$$\begin{aligned} \frac{k}{2} \mathbf{r}_{\eta\eta} \cdot (\hat{I}_s - \hat{I}_i) &= \frac{km}{2} \varsigma_{\eta\eta}(0) \hat{N} \cdot (\cos \theta^* \hat{N}) \\ &= \frac{km}{2} \frac{d^2 \mathbf{r}}{ds_{\perp}^2} \cos \theta^* \cdot \hat{N} \\ &= \frac{km}{2} \kappa \cos \theta^* \end{aligned} \quad (40a)$$

and an additional dependence on κ_{\perp} occurs through the parameter a . (See eqs. (40a) and (40b).)

Furthermore, for the reflected ray that satisfies the reflection law (eq. (1)),

$$\hat{I}_a = \hat{N}$$

consequently,

$$\cos \phi_{\parallel} = 0$$

in equation (36) and therefore, $B = 0$ (eqs. (37a) and (37b)). In this case, the factor involving the Airy function in equation (54) becomes

$$\frac{1}{(3A)^{1/3}} Ai[0] = \frac{1}{3A^{1/3} \Gamma(2/3)} \quad (55)$$

Now consider the case for which the surface is inflected in the \hat{e}_{\perp} direction. An analysis similar to the preceding one leads to a result like equation (54) with ξ, η variables interchanged and κ_{\perp} replaced by κ_{\parallel} . A difference in the physical phenomena, however, should be noted. For this case, the reflection shadow occurs because of the inflection in the \hat{e}_{\perp} direction, and consequently the incidence-reflection plane is the boundary of the shadow region. In order to compute scattering into this shadow zone, one must treat those scattering directions for which $b \neq 0$, that is, for which the factor $e^{-jb^2/4a}$ occurs in the field equation. For the previous case, on the other hand, one can study the diffraction into the shadow region for scattering directions in the incidence-reflection plane.

Location of Inflection Points

For the far-field monostatic problems, specular points are normally located by comparing the local surface normal vector \hat{N} with the reflection direction \hat{I}_r . For the corresponding bistatic problem, \hat{N} is compared with the direction of $\hat{I}_r - \hat{I}_i$. To determine whether a specular point is elliptic, parabolic, or hyperbolic, the sign of the total curvature (or equivalently, the quantity $eg - f^2$) is required. For the general scattering problem, it is advantageous to know the distribution of parabolic and hyperbolic points on the surface. This distribution can be determined by making an orderly survey of the quantity $eg = -f^2$ over the surface. Its zeros determine the lines of parabolic points which separate the hyperbolic regions from the elliptic regions.

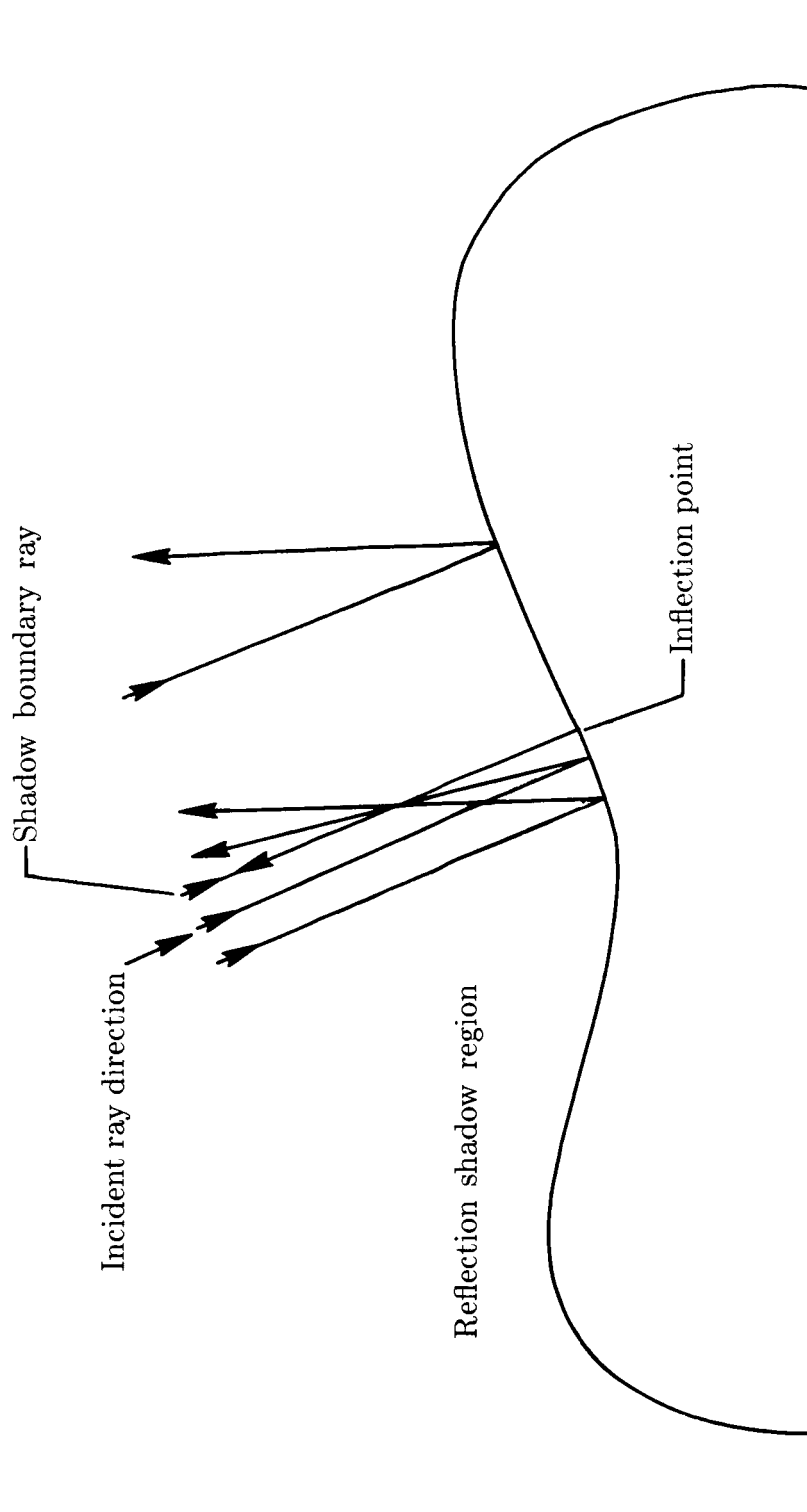
Figure 4 shows a surface having both elliptic and hyperbolic regions, with the line of parabolic points separating them.

Concluding Remarks

A theory has been presented for computing the reflected or scattered field from a smooth body with inflection points. Although the analysis was developed for electromagnetic waves, the results can easily be reduced to apply to the acoustic problem. Far-field conditions were assumed. The only restriction regarding surface geometry, other than its smoothness, was that it can be represented, at least locally, as a vector function of two variables.

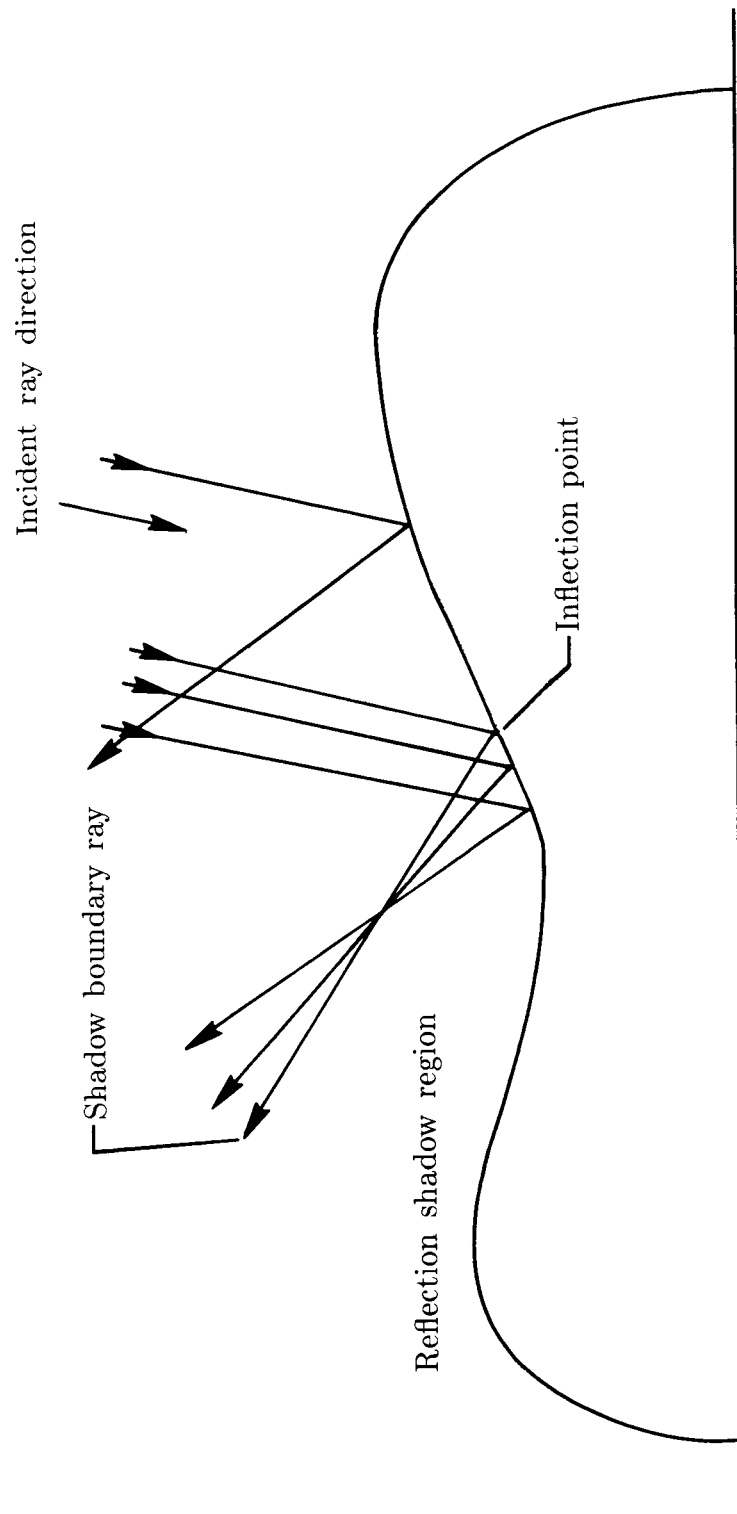
References

1. Rahnavard, Mohammad H.; and Rusch, Willard V. T.: Surface-Curvature-Induced Microwave Shadows. *IEEE Trans. Antennas & Propag.*, vol. AP-30, no. 1, Jan. 1982, pp. 83-88.
2. Barger, Raymond L.; and Adams, Mary S.: *Semianalytic Modeling of Aerodynamic Shapes*. NASA TP-2413, 1985.
3. Ludwig, Donald: Uniform Asymptotic Expansions at a Caustic. *Comm. Pure & Appl. Math.*, vol. XIX, no. 2, May 1966, pp. 215-250.
4. Struik, Dirk J.: *Differential Geometry*. Addison-Wesley Pub. Co., Inc., c.1950.
5. Silver, Samuel, ed.: *Microwave Antenna Theory and Design*. McGraw-Hill Book Co., Inc., 1949.
6. Abramowitz, Milton; and Stegun, Irene A., eds.: *Handbook of Mathematical Functions With Formulas, Graphs, and Mathematical Tables*. John Wiley & Sons, Inc., 1964. (Reprinted with corrections Dec. 1972.)



(a) Monostatic.

Figure 1. Diagram indicating reflection shadow formation at inflection point.



(b) Bistatic.

Figure 1. Concluded.

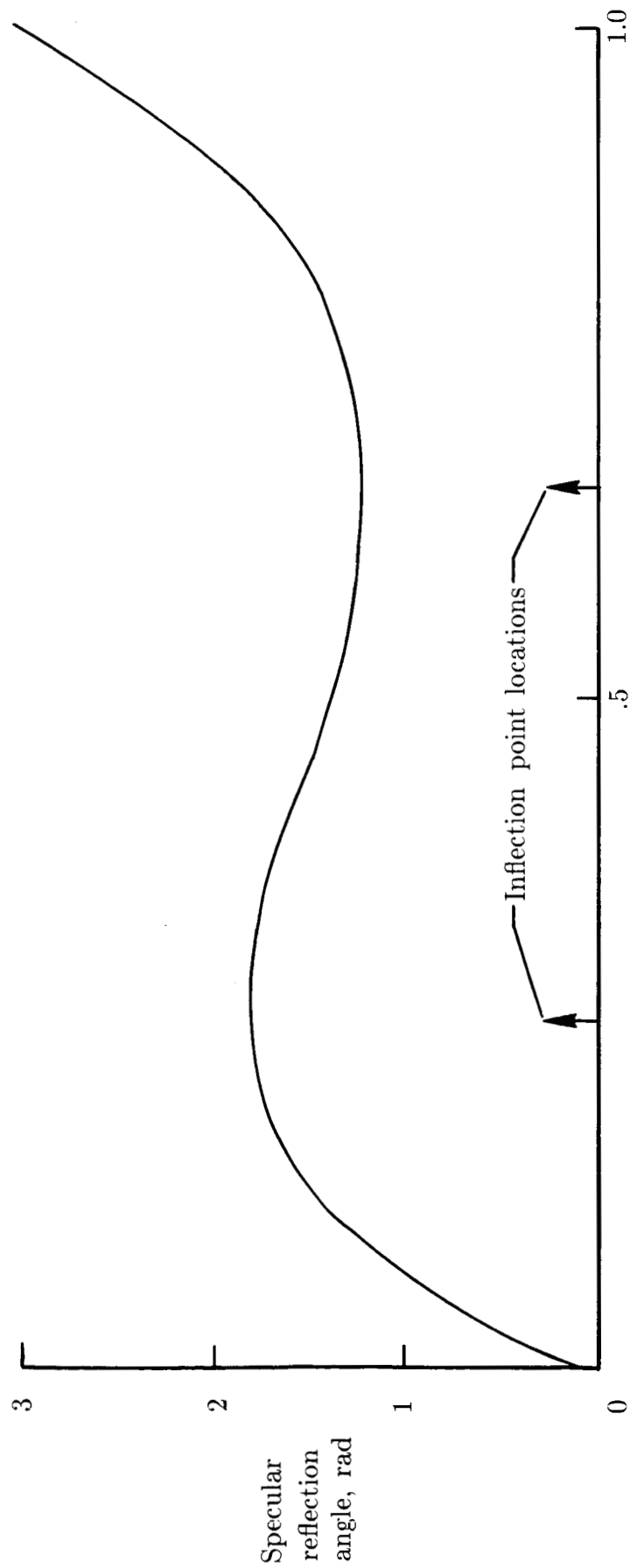


Figure 2. Distribution of specular reflection angles for body of figure 1.

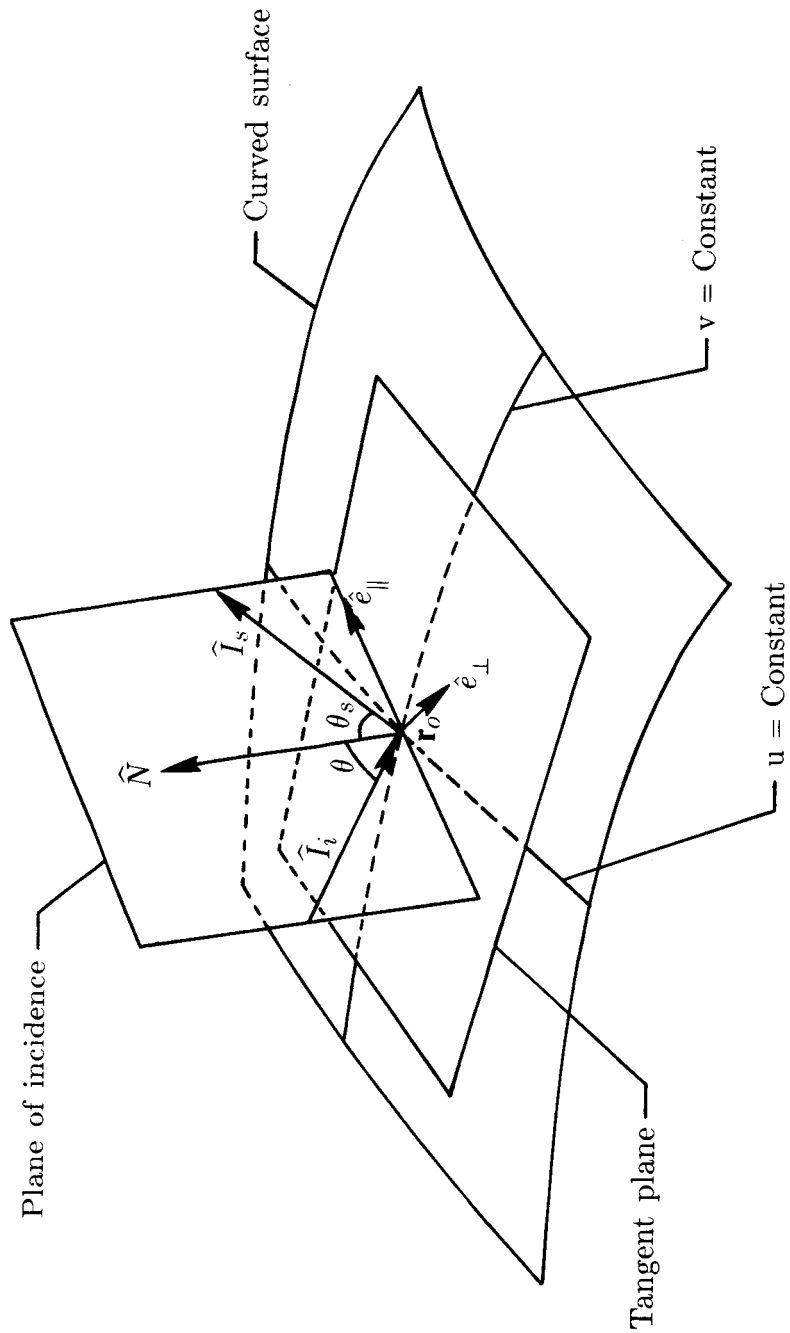


Figure 3. Geometry at point of ray incidence \mathbf{r}_o .

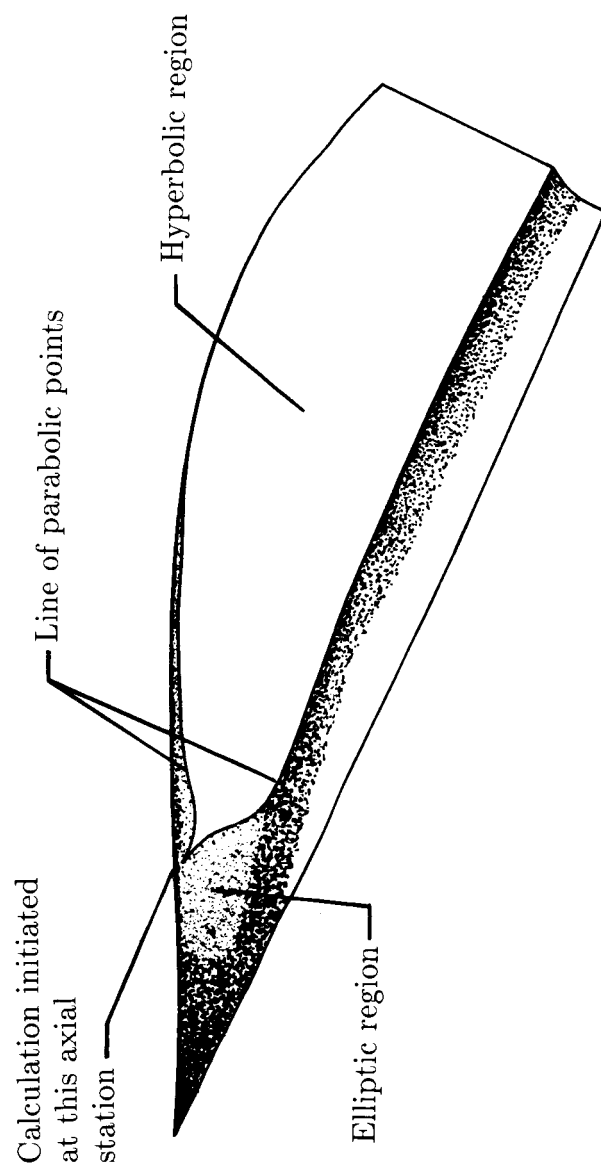


Figure 4. Infected surface showing line of parabolic points.

Standard Bibliographic Page

1. Report No. NASA TP-2632		2. Government Accession No.		3. Recipient's Catalog No.	
4. Title and Subtitle Theory for Computing the Field Reflected From a Smooth Inflected Conducting Surface				5. Report Date December 1986	
				6. Performing Organization Code 505-68-91-09	
7. Author(s) Raymond L. Barger and Allen K. Dominek				8. Performing Organization Report No. L-16157	
				10. Work Unit No.	
9. Performing Organization Name and Address NASA Langley Research Center Hampton, VA 23665-5225				11. Contract or Grant No.	
				13. Type of Report and Period Covered Technical Paper	
12. Sponsoring Agency Name and Address National Aeronautics and Space Administration Washington, DC 20546-0001				14. Sponsoring Agency Code	
15. Supplementary Notes Raymond L. Barger: Langley Research Center, Hampton, Virginia. Allen K. Dominek: Ohio State University, Columbus, Ohio.					
16. Abstract A theory is described for computing the reflected or scattered field from a smooth body with inflection points. These inflections occur in certain directions at each surface point for which the total (Gaussian) curvature is zero or negative. For surface illumination in one of these critical directions, the usual reflection formulas obtained by the high-frequency approximation are inapplicable, and a shadow zone exists in the reflected field. Scattering into the shadow zone is treated, as well as specular reflection. This theory should have a variety of applications such as for certain optics problems, computer graphics modelling of three-dimensional shapes, and the design and analysis of specialized microwave reflector antennas.					
17. Key Words (Suggested by Authors(s)) Electromagnetic waves Reflected waves Scattered waves Stationary phase Microwave reflection			18. Distribution Statement Unclassified—Unlimited Subject Category 74		
19. Security Classif.(of this report) Unclassified		20. Security Classif.(of this page) Unclassified		21. No. of Pages 20	
				22. Price A02	